

RESEARCH ARTICLE

A Simple Novel Technique of Infrared Meibography by Means of Spectral-Domain Optical Coherence Tomography: A Cross-Sectional Clinical Study

Pietro Emanuele Napoli*, Franco Coronella, Giovanni Maria Satta, Claudio Iovino, Raffaele Sanna, Maurizio Fossarello

Department of Surgical Sciences, Eye Clinic, University of Cagliari, Cagliari, Italy

* pietronapoli@gmail.com



Abstract

Purpose

To compare a novel spectral-domain optical coherence tomography (SD-OCT) technique with traditional lid transillumination for evaluation of meibomian glands (MGs) and to assess the relation of MG morphologic changes to the glandular atrophy.

Design

Evaluation of diagnostic technology.

Participants

Sixty-one patients with obstructive MGD (30 men, 31 women; age [mean ± standard deviation] 45.1 ± 12.1 years), and 75 control subjects (32 men, 43 women; 44.1 ± 12.5 years) were recruited in order to have a balanced distribution of glandular features.

Methods

Agreement between SD-OCT and lid transillumination examination for the detection of drop-out (partial or complete loss of MGs) and microscopic changes (i.e. shortening, distortion, segmentation and entanglement), as well as the relationship between morphological features and MG atrophy were evaluated.

Main Outcome Measures

Agreement between the two meibographic techniques, bias in symmetry of classification, and association analysis between microscopic changes and MG dropout.

OPEN ACCESS

Citation: Napoli PE, Coronella F, Satta GM, Iovino C, Sanna R, Fossarello M (2016) A Simple Novel Technique of Infrared Meibography by Means of Spectral-Domain Optical Coherence Tomography: A Cross-Sectional Clinical Study. PLoS ONE 11 (10): e0165558. doi:10.1371/journal.pone.0165558

Editor: Friedemann Paul, Charité Universitätsmedizin Berlin, GERMANY

Received: March 22, 2016

Accepted: October 13, 2016

Published: October 31, 2016

Copyright: © 2016 Napoli et al. This is an open access article distributed under the terms of the [Creative Commons Attribution License](https://creativecommons.org/licenses/by/4.0/), which permits unrestricted use, distribution, and reproduction in any medium, provided the original author and source are credited.

Data Availability Statement: All relevant data are within the paper and its Supporting Information files.

Funding: All authors have no support or funding to report.

Competing Interests: The authors have declared that no competing interests exist.

Results

Overall agreement for *all* morphological features was substantial (Cohen kappa coefficient = 0.77; $p < 0.001$), even if, the majority of disagreement occurred for cases with *segmentation*, where agreement was present in only 108 (81.82%) of 132 eyes with adequate images for interpretation, and where SD-OCT tended to diagnose more cases not detected by traditional lid transillumination (McNemar test, $p < 0.001$). Moreover, segmentation and distortion pattern negatively correlated with the degree of drop-out, whereas shortening and entanglement pattern demonstrated only a weak correlation (Spearman's ρ was -0.691, -0.491, -0.359, -0.385, respectively).

Conclusions

Each method has its advantages but in general there was close agreement between these meibographic techniques, particularly for MG dropout, which supports the reliability of our novel, simple and patient-friendly SD-OCT approach.

Introduction

Meibomian glands (MGs) secrete a lipid substance, i.e. the *meibum*, which retards tear evaporation and functions as lubricants for the eyelids during blinking [1,2]. In case of absence or altered integrity of meibum, the health status of the tear film and ocular surface may change, potentially causing ocular discomfort and ocular surface disease [3,4].

Obstructive meibomian gland dysfunction (MGD) is the most common cause of lipid layer deficiency and evaporative dry eye, and often results in increased tear evaporation, decreased tear stability, loss of lubrication, and damage to the ocular surface epithelium [5,6]. Molinari and Stanek reported the prevalence of MGD to be 33% in patients younger than 30 years and 71.7% in individuals 60 years or older [7].

In clinical practice, there are several methods for assessment of MG status and function, such as slit-lamp examination of the lid margins and ocular surface epithelium, meibometry, evaluation of meibum properties, and meibography [8–14]. Among them, meibography is the only approach that can show some important details of the silhouette of MGs, i.e. structural appearance and atrophy [15]. In particular, it has been shown that some morphological features of MGs, i.e. drop-out, shortening and distortion, are significantly associated with MGD [16]. For all these reasons, the practice of lid transillumination for observing MG rows remains a key technique (conventional or standard technique) in studying atrophic processes involving MGs, as well as their gross and microscopic changes [17–18].

However, although meibography was developed > 30 years ago, it is not widely used, probably because of necessary of examiner expertise as well as equipment dedicated to this analysis, which may be available only in specialized centers. Also, ocular irritation (e.g. discomfort and/or pain) induced by direct application of probe to the eyelid in transillumination systems may be a cause of the limited use of all systems of *contact meibography* [15,16].

To solve these problems, the authors introduced for the first time a simple *image processing technique* to obtain a noncontact, patient-friendly, infrared meibography by means of spectral-domain optical coherence tomography (IRM-OCT), i.e. by using the commercially available, *built-in software* to elaborate OCT images. It is interesting to note that, unlike traditional meibographic approaches, spectral-domain OCT became in the past decade one of the most widely

used device in ophthalmology imaging technology for its high resolution and fast *scan-speed* (greater than time-domain OCT). Accordingly, with our IRM-OCT technique may be not necessary a meibographic system exclusively *dedicated* to MGs examination, since spectral-domain OCT can be also available to detect details of others ocular tissues in both anterior and posterior segment of eye [19–23].

The goal of this study was therefore to describe a novel technique of IRM-OCT and to determine the level of agreement between this approach and standard meibography (traditional contact method) in patients with MGD and control subjects for the detection of a number of conventional and new MGs morphological findings. We also investigated the relation of the morphological changes to the glandular atrophy, as detected by IRM-OCT.

Methods

Subjects and examinations

This study was approved by the Office of Research Ethics, University of Cagliari, (protocol number: 2014/2682) and it adhered to the tenets of the Declaration of Helsinki. Written informed consent was obtained from all subjects before examination.

Patients presenting with complaints of ocular irritation at the Eye Clinic, who had no history of Stevens-Johnson syndrome, Sjögren's syndrome, systemic drugs use, contact lens wear, chemical, thermal, and radiation injury, or had not undergone any procedure or ocular surgery that would create an ocular surface problem, were considered to be potential participants of the study.

All physicians (PEN, FC, GMS) who examined study participants were specialists in the field of ocular surface. Data were obtained from the right eye of each subject. Examinations were performed sequentially as follows: clinical history, McMonnies questionnaire, slit-lamp observation of lid margin abnormalities and the ocular surface, fluorescein break-up time (FBUT), fluorescein staining of the cornea and conjunctiva graded according to the Oxford system, observation of the MGs in the upper and lower eyelids using lid transillumination (i.e. *contact meibography*) and using a novel OCT technique (i.e. *noncontact infrared meibography*), Schirmer I test, and evaluation of meibomian secretion (meibum) after digital pressure application on the upper lid tarsus [18–24]. Examinations were completed on the same day, generally within 25–30 minutes (~ 2–3 minutes for IRM-OCT, ~ 5–6 minutes for transillumination biomicroscopy). Assessment of the total area of the MGs in the everted eyelid (upper or lower) was performed, acquiring *three* scans (central, temporal and nasal) with IRM-OCT, and *six* or *seven* images (depending on the eyelid dimensions) with conventional meibography (since the transillumination area is small) [18,24].

After these clinical examinations, the candidate subjects were classified into 2 groups. The control group included subjects who fulfilled the following criteria: (1) McMonnies score < 10, (2) no tear film abnormalities (FBUT \geq 5 seconds and Schirmer I test value \geq 5 mm), and (3) no abnormalities of the lid margin or meibum [19,20].

The MGD group included subjects who fulfilled the diagnostic criteria for obstructive MGD: (1) chronic ocular discomfort (McMonnies questionnaire score > 10, including the positive score obtained by questions about symptoms n.5 and n.6), (2) at least one anatomic abnormalities around the meibomian gland orifices (irregularity of the lid margin, vascular engorgement, displacement of the mucocutaneous junction), (3) decreased meibum expression and obstructive findings of gland orifices [25].

Individuals whose eyes had excessive meibomian lipid secretion (seborrheic MGD), congenital deficiency of MGs, ocular allergies or any ocular disease potentially affecting tear film production or function, were excluded.

Our study groups comprised 61 patients with obstructive MGD (45.1 ± 12.1 years [mean \pm SD], 50.8% female), and 75 controls (44.1 ± 12.5 years, 57.3% female). Subjects selection and clinical/instrumental exams were performed from January 2015 to September 2015.

FBUT and fluorescein ocular surface staining

The standard FBUT measurement was performed after instillation of a 5 μ l sample of 2% fluorescein preservative-free solution in the conjunctival sac with a micropipette. After instillation, a yellow filter (Kodak Wratten no. 12) was used to enhance contrast when assessing FBUT (within 10–30 sec) and staining of the ocular surface (within 1–2 min) with a biomicroscope ($\times 10$ objective, under blue-light illumination) [5]. The patients were instructed to blink several times for a few seconds to ensure adequate mixing of the dye. The interval between the last complete blink and appearance of the first dry spot at the center of the cornea was timed using a chronometer. Three evaluations of FBUT were conducted, and the mean value was taken for data analysis [26]. The extent of the corneal surface area stained was graded according to the Oxford system [5].

Meibography by lid transillumination (standard meibography)

Meibography was performed, similarly to others, by using a transillumination device for vitrectomy with a fiberoptic light source (Millenium system, Bausch & Lomb[®], San Leandro, CA, USA) with a 20-gauge disposable fiber light guide [24].

Novel technique of noncontact infrared meibography by means of spectral-domain OCT

All images of MGs were acquired by using a commercially available OCT device, Cirrus[™] HD-OCT 4000 (Carl Zeiss Meditec Inc., Dublin, California, USA), without causing patient discomfort. This imaging system is a spectral-domain OCT platform that works at a wavelength of 840 nm, takes 27,000 axial scans per second, and has a 5- μ m axial resolution. The upper and lower eyelids were gently everted, taking care to expose palpebral conjunctiva as perpendicular as possible to the observer's line of sight (when looking straight ahead), and meibomian glands imaged, despite being only superficially visible (Fig 1). The Anterior Segment 5 Line Raster scanning protocol was used to generate all infrared images. Scans were repeated until an image of satisfying quality was obtained.

Using the *built-in software* for enhancing or reducing the contrast and/or brightness of scanned images, a single analyzer (PEN) applied the *image processing protocol* as described step-by-step in details in Table 1 and Fig 1. Each scan was interpreted by a second observer, who was masked to the study, that assessed the quality of the IRM-OCT images as either adequate or *unreadable* (i.e. uninterpretable) and recorded the conjunctival reflection as mild, fair, or excessive.

Meibographic image analysis

Each participant was *independently* examined by 1 of 2 ocular surface experts (F.C. or G.M.S.), who performed both contact and noncontact meibographic techniques (Fig 2). Immediately after meibographic examination, the chart note from that day was reviewed by the study coordinator (P.E.N.).

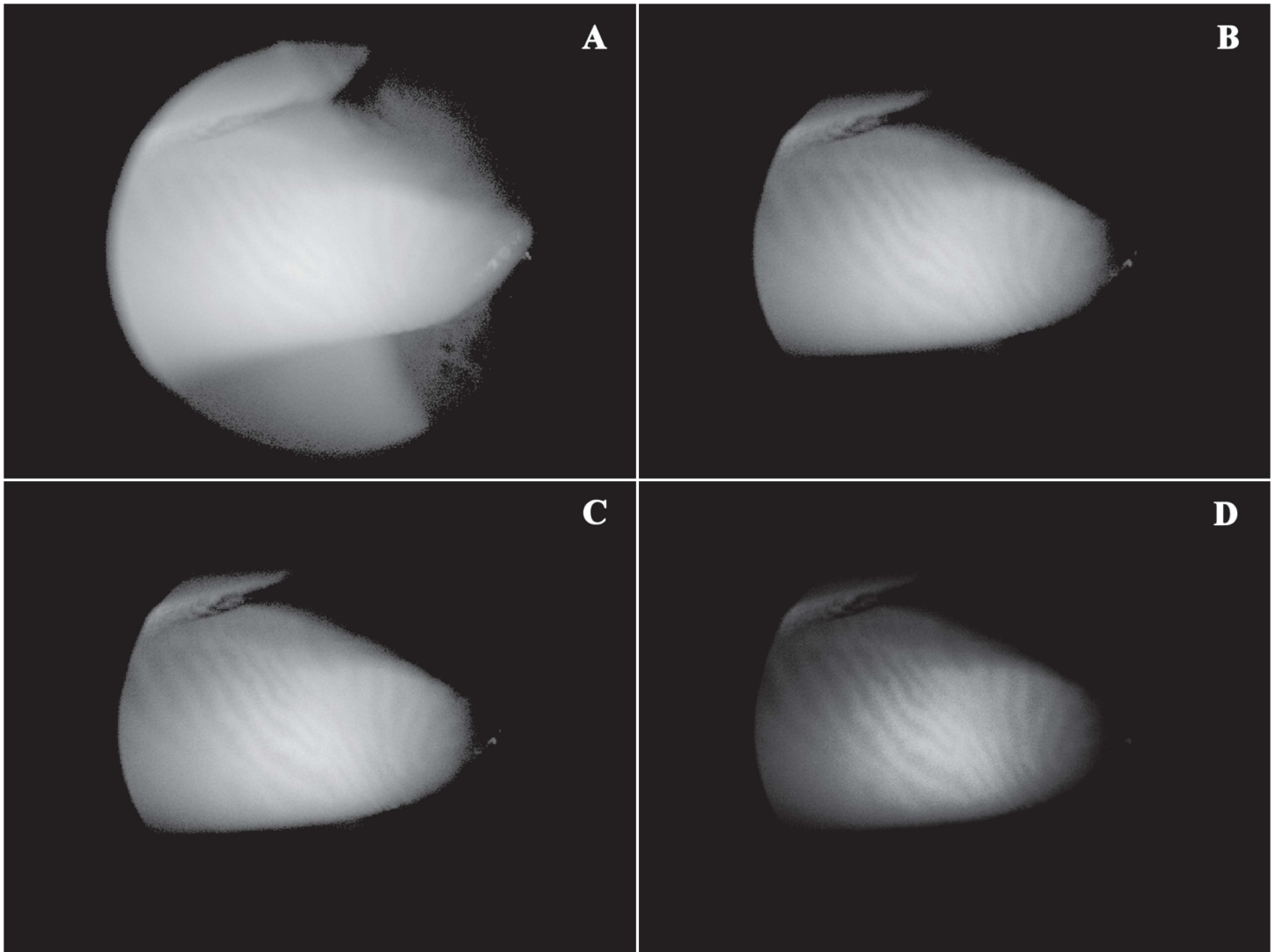


Fig 1. Image processing protocol for the detection of the meibomian glands by optical coherence tomography. In the raw, *unmodified* infrared image on optical coherence tomography (OCT) of the everted upper lid, i.e. without contrast/brightness adjustments, the detection of meibomian glands is difficult or nearly uninterpretable (at this time, their rows are only superficially visible). Applying our very simple *image processing protocol*, infrared imaging by OCT can easily reveal the silhouette of gland structure. Specifically, after hiding navigator (A), the image of the meibomian glands has been improved by modulating the contrast (mean percentage increase \pm SD, 140.6% \pm 17.7%, B) and brightness (mean percentage decrease \pm SD, 6% \pm 4.9%, C; see also Table 1). Selecting COLOR mode, it is also possible to obtain a false-color infrared OCT image of high quality for interpretation.

doi:10.1371/journal.pone.0165558.g001

Table 1. Reference values of the *image processing protocol* for enhancing meibomian gland observation on optical coherence tomography.

| | | Mean | SD | Range | Minimum | Maximum |
|-----------|--------------|-------|------|-------|---------|---------|
| Upper lid | Brightness % | -6.0 | 4.9 | 16.0 | -12.5 | 3.5 |
| | Contrast % | 140.6 | 17.7 | 52.0 | 108.0 | 160.0 |
| Lower lid | Brightness % | -3.01 | 3.05 | 5.8 | -5.8 | 0.0 |
| | Contrast % | 87.0 | 24.5 | 57.0 | 59.0 | 116.0 |

% = respect to baseline/default values.

SD = standard deviation.

doi:10.1371/journal.pone.0165558.t001

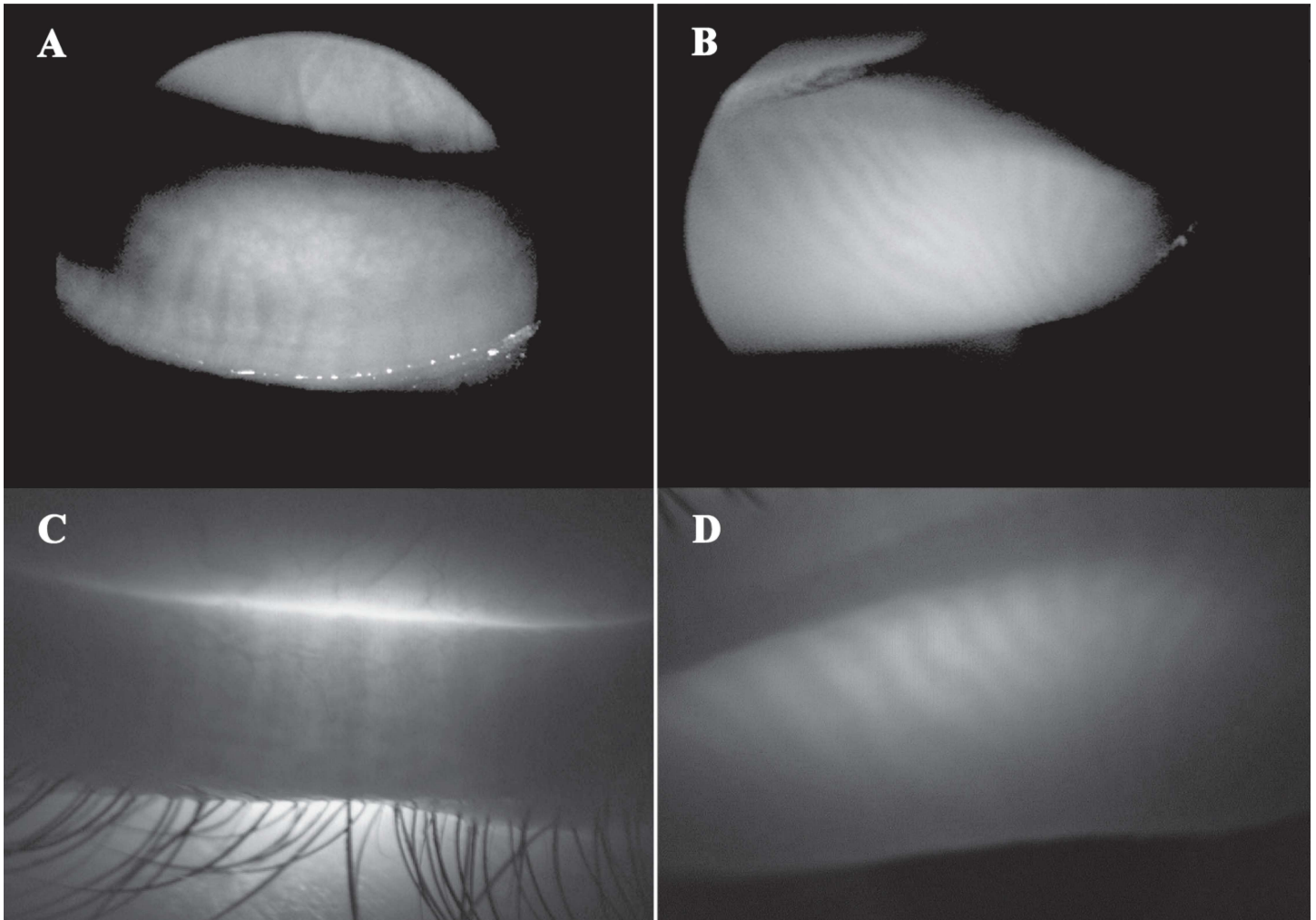


Fig 2. Meibomian glands of the lower and upper lid viewed by non-contact infrared meibography on optical coherence tomography (IRM-OCT) and transillumination meibography. The glandular architecture, i.e. acini and tubules, is revealed as a hyper-reflective structure (patches or rows) surrounded by hypo-reflective tissue by means of IRM-OCT (A and B, respectively, lower and upper eyelid), and, conversely, as a dark structure surrounded by grey-white tissue in transillumination (C and D, respectively, lower and upper eyelid).

doi:10.1371/journal.pone.0165558.g002

Dropout or atrophy of MGs (meiboscore)

Partial or complete loss of meibomian glands was scored, in both techniques, using the following grades for each eyelid: grade 0, no loss of meibomian glands; grade 1, area loss was less than 33% of the total meibomian gland area; grade 2, area loss was between 33% and 66%; grade 3, area loss was more than 66% [17]. The meiboscores for the upper and lower eyelids were summed to obtain a score of 0 through 6 for each eye [16].

Microscopic morphological features of MGs

As previously reported, shortening and distortion were evaluated as present or not present [16]. Moreover, we also introduced two new *well-defined* parameters of MG morphology, according to the following criteria: segmentation (meibomian glands appear divided into pieces in their row, Fig 3), and entanglement (meibomian glands show a tangled pattern or/and hair-pin-loop like changes in their row, Fig 3), which were also evaluated as present or not present.

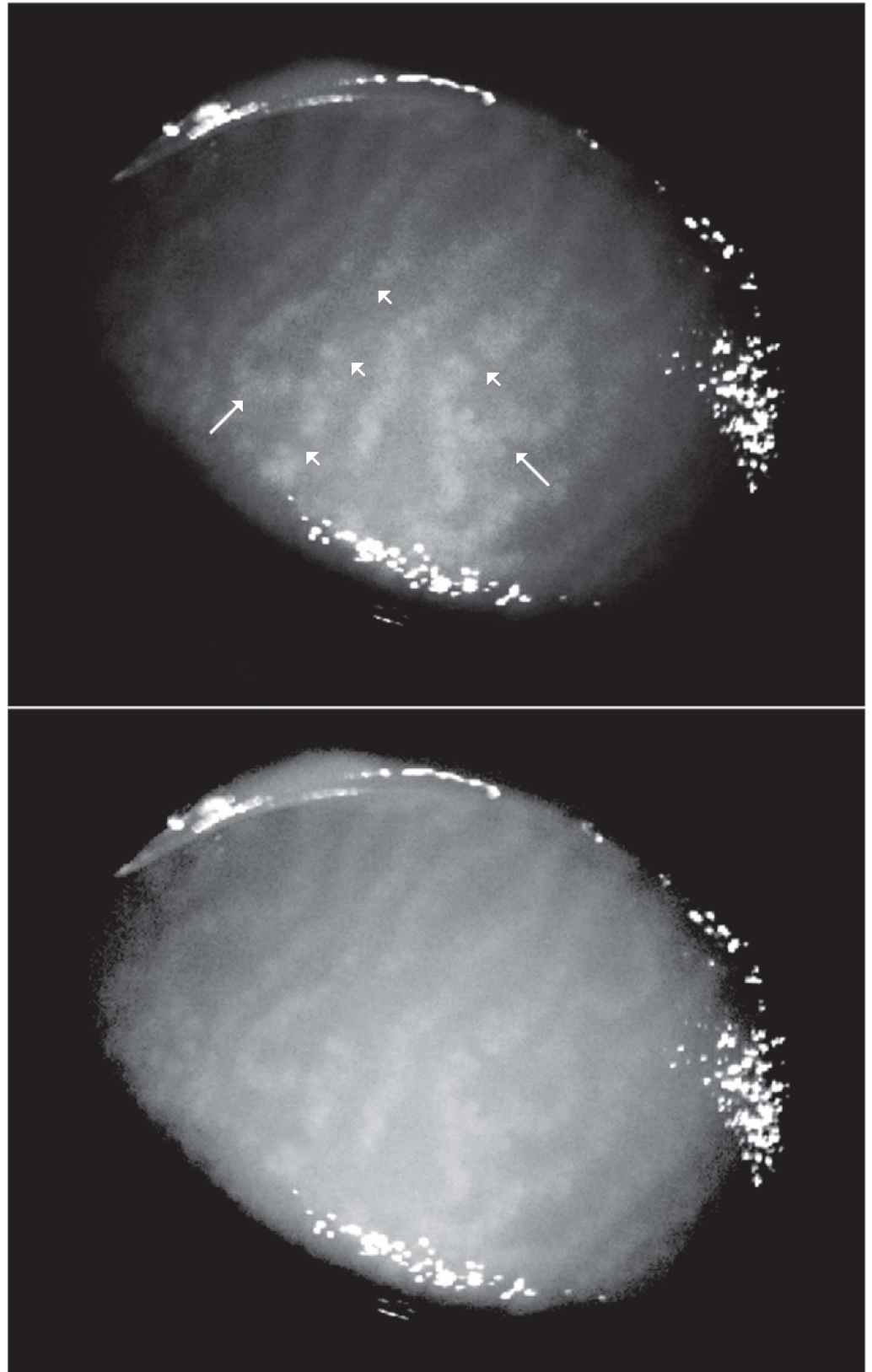


Fig 3. Non-contact infrared meibography obtained by optical coherence tomography (IRM-OCT) showing segmentation and entanglement of meibomian glands. Morphological analysis of glandular tissue may reveal micro-structural abnormalities as *segmentation*, i.e., the meibomian gland rows are divided

into pieces along their structure (short arrows), and/or *entanglement*, i.e., the meibomian gland rows show a tangled pattern or/and hairpin-loop like changes in their structure (long arrows). False-color (top) and black/white (bottom) IRM-OCT images of the same patient (34 years old, male) with meibomian gland dysfunction.

doi:10.1371/journal.pone.0165558.g003

Schirmer Test

For further evaluation of tears, the standard Schirmer I test without topical anesthesia was performed. The paper test strips (Alcon Laboratories, Fort Worth, TX) were placed over the lid margin at the junction of the lateral and middle thirds of the lower eyelid for 5 minutes. The millimeters of strip wetting were measured and recorded.

Experimental procedure

All examinations were conducted in the same conditions of temperature ($21.23 \pm 0.47^\circ\text{C}$), humidity ($40 \pm 5.72\%$) and time of the day (between 3 PM to 5 PM) in a dimly lit consulting room.

Statistical analysis

Descriptive statistics such as frequency, range, mean, and standard deviation were calculated for each characteristics.

The agreement of standard meibography versus infrared OCT meibography for each of the morphological features was assessed as the percentage agreement, and by calculating the Cohen kappa coefficient (unweighted and weighted). We also evaluated the 'overall' agreement in reporting the presence or absence of MG abnormalities, i.e. at least one of plurality of possible morphological changes (drop-out included or not). Guidelines used for interpreting the amount of agreement were those reported by Landis and Koch, where k values were defined as follows: $k = 0$ is poor agreement; $k = 0.01-0.2$ is slight agreement; $k = 0.21-0.40$ is fair agreement; $k = 0.41-0.60$ is moderate agreement; $k = 0.61-0.80$ is substantial agreement; and $k = 0.81-1.00$ is almost perfect agreement [27]. In addition, a binomial test, also known as the McNemar test, was performed as a test for bias in symmetry of the disagreements in reading of the paired images (for each parameter), and Bonferroni correction for the *post-hoc* analysis.

Relationship between presence/degree of drop-out and microscopic morphological features of MGs, as detected by IRM-OCT, was determined by calculating Pearson χ square test and Spearman's ρ test.

With an accepted alpha risk of 0.05 and a β risk of 0.20 (i.e., 80% statistical power) in a two-sided test, approximately 60 subjects are needed before a correlation coefficient of 0.35 is said to be statistically significant.

If an infrared OCT meibography image was graded as *unreadable*, then the subject's data point for both techniques was excluded from analysis of the total agreement. Statistical significance was considered if $p < 0.05$.

Results

Patient data

The demographic and clinical characteristics are summarized in Table 2 and in S1 and S2 Tables. The noncontact infrared meibographic images obtained with OCT were of sufficient quality for interpretation in 132 (97.1%) of 136 cases tested. In cases of uninterpretable images, the OCT operator attributed poor image quality to artifact due to the excessive *conjunctival reflection* (Table 3).

Table 2. Distributions of meibomian gland abnormalities as detected by meibographic techniques.

| Study participants (44.5 ± 12.3 years [mean ± SD], 54.4% female) | | |
|---|--|----------------------------|
| Detection of morphological findings | Lid transillumination No. (% of eyes) | IRM-OCT No. (% of eyes) |
| Meiboscore = 0 | 30 (22.7) | 30 (22.7) |
| Meiboscore = 1 | 48 (36.4) | 48 (36.4) |
| Meiboscore = 2 | 30 (22.7) | 30 (22.7) |
| Meiboscore = 3 | 24 (18.2) | 24 (18.2) |
| Shortening | 72 (54.5) | 72 (54.5) |
| Distortion | 84 (63.6) | 78 (59.1) |
| Segmentation | 54 (40.9) | 78 (59.1) |
| Entanglement | 36 (27.3) | 36 (27.3) |

IRM-OCT = Infrared meibography by optical coherence tomography.

SD = standard deviation.

doi:10.1371/journal.pone.0165558.t002

Drop-out (meiboscore)

Of the 132 eyes, no drop-out (meiboscore grade = 0) was present in 30 (22.7%) of the cases, as detected by both techniques. Similarly, meiboscore grade 1, 2, and 3, were detected in 48 (36.4%), 30 (22.7%), 24 (18.2%) of the cases by transillumination biomicroscopy or by IRM-OCT. When comparing drop-out results of the two meibographic techniques, complete agreement was found in 120 (90.9%) of 132 eyes (weighted $k = 0.92$; $p < 0.001$). No discrepancy in classification was observed (McNemar test with Bonferroni correction, $p = 1.0$; Table 4).

Microscopic features

Of the 132 eyes, shortening, distortion, segmentation, and entanglement, by transillumination biomicroscopy were present in 72 (54.5%), 84 (63.6%), 54 (40.9%), 36 (27.3%) of the cases, respectively. By comparison, shortening, distortion, segmentation, and entanglement, were detected by IRM-OCT in 72 (54.5%), 78 (59.1%), 78 (59.1%), 36 (27.3%) eyes, respectively. Individually, the clinical presence of each microscopic feature demonstrated substantial to almost perfect agreement between results of transillumination biomicroscopy and IRM-OCT ($k = 0.81$; $k = 0.71$; $k = 0.64$; $k = 0.77$; $p < 0.001$, for shortening, distortion, segmentation, and entanglement, respectively). Overall agreement for microscopic features was substantial ($k = 0.76$; $p < 0.001$). However, the majority of disagreement occurred for cases with segmentation, where agreement was present in only 108 (81.82%) of 132 eyes, and where IRM-OCT tended to diagnose more ‘aggressively’ its presence (McNemar test, $p < 0.001$; Table 4).

Table 3. Cross-tabulation frequency of the quality of images for interpretation by reflection artifacts.

| | | Conjunctival reflection (artifact) | | | |
|---|------------------------|------------------------------------|--------------------|------------------|------------------|
| | | none | mild | fair | excessive |
| IRM-OCT images (quality for interpretation) | Adequate ($n = 132$) | 78% ($n = 106$) | 14.7% ($n = 20$) | 4.4% ($n = 6$) | 0% ($n = 0$) |
| | Unreadable ($n = 4$) | 0% ($n = 0$) | 0% ($n = 0$) | 0% ($n = 0$) | 2.9% ($n = 4$) |

IRM-OCT = Infrared meibography by optical coherence tomography.

doi:10.1371/journal.pone.0165558.t003

Table 4. Agreement in meibomian gland detection of morphological changes between meibographic techniques.

| | Percentage Agreement No. (% of eyes) | Agreement (Kappa) ^a 95%CI | Bias in symmetry (p-value) ^b |
|------------------------------|---|---|--|
| Drop-out (meiboscore) | 120 (90.9) | 0.92 ^c (0.84–0.99) | 1.0 ^d |
| Shortening | 120 (90.9) | 0.81 (0.57–0.93) | 1.0 |
| Distortion | 114 (86.3) | 0.71 (0.54–0.84) | 0.23 |
| Segmentation | 108 (81.8) | 0.64 (0.48–0.79) | <0.001 |
| Entanglement | 120 (90.9) | 0.77 (0.61–0.92) | 1.0 |
| Microscopic features* | 116 (87.8) | 0.76 (0.55–0.87) | 0.01 |
| All morphological features** | 117 (88.6) | 0.77 (0.6–0.89) | 0.02 |

^a Cohen’s kappa; $p < 0.001$ for all comparisons shown.

^b McNemar test (binomial distribution used).

^c Cohen’s kappa, weighted; $p < 0.001$.

^d Bonferroni correction for *post-hoc* analysis.

* = detection of at least one of the following morphological findings: shortening / distortion / segmentation / entanglement.

** = detection of dropout or/and microscopic features.

doi:10.1371/journal.pone.0165558.t004

All morphological features

Overall agreement for *all* morphological features was substantial ($k = 0.77$; $p < 0.001$, please see [Table 4](#)).

Association analysis

A statistically significant relationship was found between presence of drop-out and shortening, distortion, segmentation, or entanglement (Pearson χ square tests, $p < 0.001$, please see [Table 5](#)). Interestingly, segmentation and distortion pattern negatively correlated with the degree of drop-out, whereas shortening and entanglement pattern demonstrated only a weak correlation (Spearman’s ρ was -0.691, -0.491, -0.359, -0.385, respectively, please see [Table 5](#)).

Discussion

Traditional methods available for directly studying the architecture of MGs are meibography and biopsy [18]. Clearly, biopsy may reveal microscopic features of glandular structure, but it is an invasive *ex vivo* analysis and patients are frequently reluctant to consent to such

Table 5. Association and correlation analysis between atrophic processes and microscopic morphological features.

| | Drop-out (atrophy) detection | |
|--------------|------------------------------|-------------------|
| Shortening | $\chi = 52.140^a$ | $\rho = -0.359^*$ |
| Distortion | $\chi = 42.361^b$ | $\rho = -0.491^*$ |
| Segmentation | $\chi = 54.688^c$ | $\rho = -0.691^*$ |
| Entanglement | $\chi = 20.075^d$ | $\rho = -0.385^*$ |

χ = Pearson Chi-Square; $p < 0.001$ for all associations shown.

ρ = Spearman Correlation;

^{a, b, c, d} Zero cells (0.0%) have expected count less than 5. The minimum expected count is 10.91, 8.79, 8.79, 6.55, respectively.

* Based on normal approximation.

doi:10.1371/journal.pone.0165558.t005

procedure. In contrast, a number of contact and non-contact meibographic systems may permit a non-invasive *in vivo* study through direct observation of gross and microscopic features of the silhouette of MGs. Nevertheless, although MGD is one of the most common abnormalities in ophthalmic practice as well as the major cause of evaporative dry eye, or meibography represents the most important diagnostic approach for MGs observation, morphological evaluation of MGs is performed only in a limited number of clinics [16,17].

In the present study, we introduce a simple, novel technique to obtain a noncontact infrared meibography by a commercially available spectral-domain OCT system, which is, to date, one of the most widely used tool in diagnostic imaging in ophthalmology. Using our procedure, the architecture of glandular rows is easily visible in both upper and lower eyelid within 2–3 minutes, without all disadvantages of traditional methods. In particular, patients discomfort induced by the direct application of the transilluminating light probe (contact meibography), or the need for an *expensive/dedicated* noncontact meibographic system, for an *indirect digitization* of MGs images, or the topical anesthesia before the invasive alignment of the device lens directly against the everted eyelid (e.g., as in case of meibography obtained by confocal microscopy), are all limits addressed by our method.

Unlike OCT tomograms of MGs previously reported [28–29], our IRM-OCT approach utilizes a standard, commercially available spectral-domain OCT, which is faster than a time-domain (i.e. Visante OCT), and it doesn't require an *external software* to elaborate images (but only the commercially available, *built-in software* to elaborate OCT images), thereby leading an easier, less time-consuming examination.

The authors believe that the method proposed herein is a useful, outstanding, simple approach to allow meibography to be truly a widespread, routine examination in clinical and research use. In fact, although spectral-domain OCT working at a wavelength of 840 nm (840-nm OCT) was primarily developed to evaluate posterior segment [30], its infrared signal is able to *noninvasively* detect MGs for their peculiar peak of absorbance, related to the tubulo-acinar wall and/or to their lipid content, which appear different from the fibrous tarsus.

With regard to the agreement results, the nearly equal numbers of men and women, inclusion of normal subjects and patients with both microscopic morphological features and MG drop-out, as well as the relatively balanced distribution of glandular atrophic levels supports the external validity of our findings. Although lid transillumination represents a standard technique of contact meibography, its use may still currently provide a non-expensive, well-recognized approach for a number of countries in the world. On the other hand, our technique doesn't involve any additional cost in diagnostic departments where there is a similar OCT system. Overall, we found substantial agreement between standard meibography and our IRM-OCT method for the detection of all morphological features. Individually, each parameter showed substantial to almost perfect agreement in results between the two techniques, except for segmentation, where bias in symmetry was found to be statistically significant. The failure of standard meibography to strongly correlate with segmentation detected by IRM-OCT in this study suggests that our technique may be more sensitive not only in revealing to such alteration in patients with MGD, but also in detecting a thinning/interruption of glandular wall along MG rows, or a non-homogeneous distribution of lipids in the glandular lumen. We believe that a similar finding may be important for an early diagnosis of subtle morphological alterations of glandular structure during obvious and non-obvious MGD, as well as for a more accurate follow-up.

To further investigate the morphological abnormalities in the MGs, we introduced for the first time two new *well-defined* parameters, segmentation and entanglement. To our surprise, eyes with presence of MG drop-out (grade 1, 2, 3) were significantly associated with entanglement of MG structure, which indicates that atrophic processes may alter the regular

architecture of the MGs at any stage of evolution. In contrast, the segmentation pattern was mainly observed in patients with lower drop-out grades, suggesting that the destructive process of glandular rows implies their early fragmentation, which is easily detectable by 840-nm infrared OCT. From a theoretical point of view, segmentation and entanglement are two promising new parameters for evaluating MGD. In this sense, IRM-OCT could effectively demonstrate early abnormalities in glandular morphology before extensive and/or obvious atrophy in their area.

In general, since MGD may be associated with increased risk of ocular complications, i.e. contact lens intolerance and/or discontinuation of contact wear, ocular allergies and ocular surface diseases (e.g., pterygium), discomfort after visual display terminal (VDT) usage, intolerance to glaucoma medications, unsatisfactory refractive surgery outcomes, post-cataract endophthalmitis, etc. the authors firmly believe that IRM-OCT could truly help ophthalmologists in the assessment for prevention and management of all these conditions [31–37].

There are some limitations to the present study. First, although our technique permits direct observation of MGs on OCT, without exporting and processing OCT images with an additional/external software, it implies *manual* adjustments of images according to the reference values described above. Future studies should introduce and evaluate a totally automatic software, which can be easily integrated on OCT systems. Second, further investigations are necessary to clarify the association of our findings with aging and gender, and the diagnostic validity of segmentation and entanglement. Third, we did not perform a comparison analysis between proximal, mid and distal parts of the glandular structure for agreement.

In summary, our novel technique may represent a useful, simple and patient-friendly approach for obtaining information on the MG structure with one of the most widely used device in ophthalmic imaging. Therefore, IRM-OCT has the potential to popularize the field of meibography, facilitating a widespread clinical and research use. Although both meibographic techniques have their advantages (i.e., standard and IRM-OCT), in general there was close agreement between these methods, particularly for MG dropout, which supports the reliability of our novel OCT approach. Specifically, compared with lid transillumination, IRM-OCT seemed more sensitive in detecting microscopic structural changes, e.g. segmentation of glandular rows.

For all these reasons, the procedure described herein may represent an easily accessible method for MG observation and enrich the diagnostic armamentarium of ophthalmologists for studying some very common ocular surface diseases (e.g., MGD, lipid layer deficiency and/or evaporative dry eye).

Supporting Information

S1 Table. Minimum data set. A table with summaries of demographic data of patients. (XLSX)

S2 Table. Descriptive statistics of patients. (DOC)

Author Contributions

Conceptualization: PEN.

Data curation: PEN FC GMS CI RS MF.

Formal analysis: PEN.

Investigation: PEN.

Methodology: PEN FC GMS CI RS.

Project administration: PEN.

Resources: PEN MF.

Software: PEN.

Supervision: PEN MF.

Validation: PEN FC GMS CI RS MF.

Visualization: PEN FC GMS CI RS MF.

Writing – original draft: PEN.

Writing – review & editing: PEN MF.

References

- Mishima S, Maurice DM (1961) The oil layer of the tear film and evaporation from the corneal surface. *Exp Eye Res* 1: 39–45. PMID: [14474548](#)
- Bron AJ, Tiffany JM, Gouveia SM, Yokoi N, Voon LW (2004) Functional aspects of the tear film lipid layer. *Exp Eye Res* 78: 347–360. PMID: [15106912](#)
- Foulks GN (2007) The correlation between the tear film lipid layer and dry eye disease. *Surv Ophthalmol* 52: 369–374. doi: [10.1016/j.survophthal.2007.04.009](#) PMID: [17574063](#)
- Breustedt DA, Schonfeld DL, Skerra A (2006) Comparative ligand binding analysis of ten human lipocalins. *Biochim Biophys Acta* 1764: 161–173. doi: [10.1016/j.bbapap.2005.12.006](#) PMID: [16461020](#)
- Methodologies to diagnose and monitor dry eye disease: Report of the Diagnostic Methodology Subcommittee of the International Dry Eye Workshop (2007) *Ocul Surf* 5: 108–152. PMID: [17508118](#)
- Tomlinson A, Bron AJ, Korb DR, Amano S, Paugh JR, Pearce EI, et al. (2011) The International Workshop on Meibomian Gland Dysfunction: Report of the Diagnosis Subcommittee. *Invest Ophthalmol Vis Sci* 52: 2006–2049. doi: [10.1167/iov.10-6997f](#) PMID: [21450918](#)
- Molinari JF, Stanek S. (2000) Meibomian gland status comparison between active duty personnel and U.S. veterans. *Mil Med* 165: 591–593. PMID: [10957850](#)
- Chew CK, Jansweijer C, Tiffany JM, Dikstein S, Bron AJ. (1993) An instrument for quantifying meibomian lipid on the lid margin: the Meibometer. *Current Eye Res* 12: 247–254.
- Yokoi N, Mossa F, Tiffany JM, Bron AJ. (1999) Assessment of meibomian gland dysfunction in dry eye using meibometry. *Arch Ophthalmol* 117: 723–729. PMID: [10369581](#)
- Tapie R. (1977) Biomicroscopical study of Meibomian glands [in French]. *Ann Ocul (Paris)* 210: 637–648.
- Robin JB, Jester JV, Nobe J, Nicolaidis N, Smith RE. (1985) In vivo transillumination biomicroscopy and photography of meibomian gland dysfunction: a clinical study. *Ophthalmology* 92: 1423–1426. PMID: [4069605](#)
- Mathers WD, Daley T, Verdick R. (1994) Video imaging of the meibomian gland [letter]. *Arch Ophthalmol* 112: 448–449.
- Yokoi N, Komuro A, Yamada H, Maruyama K, Kinoshita S (2007) A newly developed video-meibography system featuring a newly designed probe. *Jpn J Ophthalmol* 51: 53–56. doi: [10.1007/s10384-006-0397-y](#) PMID: [17295142](#)
- Nichols JJ, Berntsen DA, Mitchell GL, Nichols KK. (2005) An assessment of grading scales for meibography images. *Cornea* 24: 382–388. PMID: [15829792](#)
- Arita R, Zavala M, Yee RW (2014) MGD Diagnosis. *Current Ophthalmol Rep* 2(2): 49–57.
- Arita R, Itoh K, Maeda S, Maeda K, Furuta A, Fukuoka S, et al. (2009) Proposed diagnostic criteria for obstructive meibomian gland dysfunction. *Ophthalmology* 116: 2058–2063. doi: [10.1016/j.ophtha.2009.04.037](#) PMID: [19744718](#)
- Arita R, Itoh K, Inoue K, Amano S (2008) Noncontact infrared meibography to document age-related changes of the meibomian glands in a normal population. *Ophthalmology* 115: 911–915. doi: [10.1016/j.ophtha.2007.06.031](#) PMID: [18452765](#)

18. Wise RJ, Sobel RK, Allen RC (2012) Meibography: A review of techniques and technologies. *Saudi J Ophthalmol* 26: 349–356. doi: [10.1016/j.sjopt.2012.08.007](https://doi.org/10.1016/j.sjopt.2012.08.007) PMID: [23961019](https://pubmed.ncbi.nlm.nih.gov/23961019/)
19. Napoli PE, Coronella F, Satta GM, Fossarello M (2014) A Novel Technique of Contrast-Enhanced Optical Coherence Tomography Imaging in Evaluation of Clearance of Lipids in Human Tears. *PLoS One* 9(11), e109843. doi: [10.1371/journal.pone.0109843](https://doi.org/10.1371/journal.pone.0109843) PMID: [25369027](https://pubmed.ncbi.nlm.nih.gov/25369027/)
20. Napoli PE, Coronella F, Satta GM, Galantuomo MS, Fossarello M (2014) Evaluation of the Adhesive Properties of the Cornea by Means of Optical Coherence Tomography in Patients with Meibomian Gland Dysfunction and Lacrimal Tear Deficiency. *PLoS One* 9(12), e115762. doi: [10.1371/journal.pone.0115762](https://doi.org/10.1371/journal.pone.0115762) PMID: [25536051](https://pubmed.ncbi.nlm.nih.gov/25536051/)
21. Napoli PE, Coronella F, Satta GM, Zucca IA, Fossarello M (2014) A novel OCT technique to measure in vivo the corneal adhesiveness for sodium carboxymethylcellulose in humans and its validity in the diagnosis of dry eye. *Invest Ophthalmol Vis Sci* 55: 3179–3185. doi: [10.1167/iovs.13-13613](https://doi.org/10.1167/iovs.13-13613) PMID: [24764061](https://pubmed.ncbi.nlm.nih.gov/24764061/)
22. Napoli PE, Satta GM, Coronella F, Fossarello M (2014) Spectral-domain optical coherence tomography study on dynamic changes of human tears after instillation of artificial tears. *Invest Ophthalmol Vis Sci* 55: 4533–4540. doi: [10.1167/iovs.14-14666](https://doi.org/10.1167/iovs.14-14666) PMID: [24985473](https://pubmed.ncbi.nlm.nih.gov/24985473/)
23. Napoli PE, Nioi M, d'Aloja E, Fossarello M (2016) Post-Mortem Corneal Thickness Measurements with a Portable Optical Coherence Tomography System: a Reliability Study. *Sci Rep* 6: 30428; doi: [10.1038/srep30428](https://doi.org/10.1038/srep30428) PMID: [27457021](https://pubmed.ncbi.nlm.nih.gov/27457021/)
24. Shimazaki J, Sakata M, Tsubota K (1995) Ocular surface changes and discomfort in patients with meibomian gland dysfunction. *Arch Ophthalmol* 113: 1266–1270. PMID: [7575257](https://pubmed.ncbi.nlm.nih.gov/7575257/)
25. Amano S (2010) MGD Working Group: Definition and diagnostic criteria for meibomian gland dysfunction. *J Eye (Atarashii Ganka)* 27: 627–631.
26. Johnson ME, Murphy PJ (2005) The effect of instilled fluorescein solution volume on the values and repeatability of FBUT measurements. *Cornea* 24: 811–817. PMID: [16160497](https://pubmed.ncbi.nlm.nih.gov/16160497/)
27. Landis JR, Koch GG (1977) The measurement of observer agreement for categorical data. *Biometrics* 33: 159–174. PMID: [843571](https://pubmed.ncbi.nlm.nih.gov/843571/)
28. Hwang HS, Shin JG, Lee BH, Eom TJ, Joo CK (2013) In vivo 3D meibography of the human eyelid using real time imaging Fourier-domain OCT. *PloS One* 8(6), e67143. doi: [10.1371/journal.pone.0067143](https://doi.org/10.1371/journal.pone.0067143) PMID: [23805297](https://pubmed.ncbi.nlm.nih.gov/23805297/)
29. Hwang HS, Chang WP, Choun-Ki J (2013) Novel noncontact meibography with anterior segment optical coherence tomography: Hosik meibography. *Cornea* 32: 40–43. doi: [10.1097/ICO.0b013e318247b2fd](https://doi.org/10.1097/ICO.0b013e318247b2fd) PMID: [22677640](https://pubmed.ncbi.nlm.nih.gov/22677640/)
30. Napoli PE, Zucca I, Fossarello M (2014) A qualitative and quantitative analysis of filtering blebs with optical coherence tomography in patients after primary trabeculectomy. *Can J Ophthalmol* 49: 210–216. doi: [10.1016/j.jcjo.2013.10.003](https://doi.org/10.1016/j.jcjo.2013.10.003) PMID: [24767231](https://pubmed.ncbi.nlm.nih.gov/24767231/)
31. Arita R, Itoh K, Inoue K, Kuchiba A, Yamaguchi T, Amano S. (2009) Contact lens waer is associated with decrease of meibomian glands. *Ophthalmology* 116: 379–384. doi: [10.1016/j.ophtha.2008.10.012](https://doi.org/10.1016/j.ophtha.2008.10.012) PMID: [19167077](https://pubmed.ncbi.nlm.nih.gov/19167077/)
32. Wu H, Wang Y, Dong N, Yang F, Lin Z, Shang X, et al. (2014) Meibomian gland dysfunction determines the severity of the dry eye conditions in visual display terminal workers. *PloS One* 9(8), e105575. doi: [10.1371/journal.pone.0105575](https://doi.org/10.1371/journal.pone.0105575) PMID: [25144638](https://pubmed.ncbi.nlm.nih.gov/25144638/)
33. Ye T, Chen W, Congdon N, Liu Y (2014) Increase in microbial contamination risk with compression of the lid margin in eyes having cataract surgery. *J Cataract Refract Surg* 40: 1377–1381. doi: [10.1016/j.jcrs.2013.11.046](https://doi.org/10.1016/j.jcrs.2013.11.046) PMID: [25088638](https://pubmed.ncbi.nlm.nih.gov/25088638/)
34. Viso E, Rodriguez-Ares MT, Bòveda FJ, Tourino R, Gude F (2014) Prevalence of conjunctival shrinkage and its association with dry eye disease: results from a population-based study in Spain. *Cornea* 33: 442–447. doi: [10.1097/ICO.0000000000000091](https://doi.org/10.1097/ICO.0000000000000091) PMID: [24622297](https://pubmed.ncbi.nlm.nih.gov/24622297/)
35. Azar D (2015) Lasik early postoperative complication refractive surprise (pp 34–70). Specific topics covered by the cases include how to manage a simple infection (Case 32), a step-by-step evolution of a severe infection (Case 33). *Difficult and Complicated Cases in Refractive Surgery* 147.
36. Chu R, Qazi MA, Pepose JS (2012) The effect of dry eye disease on vision and its implications for cataract and refractive surgery. *Ocular Surface Disorders* 69.
37. Arita R, Itoh K, Maeda S, Maeda K, Furuta A, Tomidoro A, Amano S (2010) Meibomian gland duct distortion in patients with perennial allergic conjunctivitis. *Cornea* 29: 858–860. doi: [10.1097/ICO.0b013e3181ca3668](https://doi.org/10.1097/ICO.0b013e3181ca3668) PMID: [20508507](https://pubmed.ncbi.nlm.nih.gov/20508507/)